Supplementary Material for the Paper: Directed Graph Contrastive Learning

Zekun Tong[1] **Yuxuan Liang**[1] **Henghui Ding** [2,3,*]
Yongxing Dai [4] **Xinke Li**[1] **Changhu Wang**[2]
[1]National University of Singapore [2]ByteDance [3]ETH Zürich [4]Peking University
{zekuntong,liangyuxuan,xinke.li}@u.nus.edu
henghui.ding@vision.ee.ethz.ch, yongxingdai@pku.edu.cn
changhu.wang@bytedance.com

A Proofs of Theorems

A.1 Proof of Theorems 1

THEOREM 1. ***Monotonicity of the perturbation error***. *The perturbation error $\Delta\tilde{\mathcal{H}}_{\mathrm{VN}}$ increases monotonically with the Laplacian perturbation term $\Delta\alpha$.*

Proof. The perturbation error is defined in DEFINITION (3) of the main text as

$$\Delta\tilde{\mathcal{H}}_{\mathrm{VN}}(\alpha,\alpha+\Delta\alpha)=\frac{1}{2n^2}\left\{\sum_{(u,v)\in\mathcal{E}}\left(\frac{\pi_{\mathrm{appr}}^{\alpha+\Delta\alpha}(u)}{\pi_{\mathrm{appr}}^{\alpha+\Delta\alpha}(v)d_u^{\mathrm{out}^2}}-\frac{\pi_{\mathrm{appr}}^{\alpha}(u)}{\pi_{\mathrm{appr}}^{\alpha}(v)d_u^{\mathrm{out}^2}}\right)\right\}. \tag{1}$$

We start out the proof from Eq. (1) in the main text, leading to

$$(1-\alpha)\pi_{\mathrm{appr}}^{\alpha}\tilde{\mathbf{P}}+\frac{1}{n}\frac{\alpha}{1+\alpha}\mathbf{1}^{1\times n}=\pi_{\mathrm{appr}}^{\alpha}, \tag{2}$$

and the approximate eigenvector component for node u is

$$\pi_{\mathrm{appr}}^{\alpha}(u)=(1-\alpha)\sum_{i,(i,u)\in\mathcal{E}}\pi_{\mathrm{appr}}^{\alpha}(i)\tilde{\mathbf{P}}(i,u)+\frac{1}{n}\frac{\alpha}{1+\alpha}. \tag{3}$$

In the [19], they assume that the eigenvector component is proportional to the in-degree of the corresponding node when the neighborhood of this node has similar out-degree and in-degree, *i.e.*,

$$\frac{\sum_{i,(i,u)\in\mathcal{E}}\pi_{\mathrm{appr}}^{\alpha}(i)\tilde{\mathbf{P}}(i,u)}{\sum_{i,(i,v)\in\mathcal{E}}\pi_{\mathrm{appr}}^{\alpha}(i)\tilde{\mathbf{P}}(i,v)}\approx\frac{d_u^{\mathrm{in}}}{d_v^{\mathrm{in}}}=\frac{cd_u^{\mathrm{in}}}{cd_v^{\mathrm{in}}}, \tag{4}$$

where the constant c controls the d_u^{in} and $\pi_{\mathrm{appr}}^{\alpha}(i)\tilde{\mathbf{P}}(i,u)$ at the same scale. Meanwhile, they experimentally verify that even under this strong assumption, the calculated von Neumann entropy does not show significant errors [19]. Thus, we adopt their assumption and simply Eq. (4) to

$$\sum_{i,(i,u)\in\mathcal{E}}\pi_{\mathrm{appr}}^{\alpha}(i)\tilde{\mathbf{P}}(i,u)\approx cd_u^{\mathrm{in}}. \tag{5}$$

*Corresponding author

We further let $0 < \alpha_1 < \alpha_2 < 1$ and take them into Eq. (1)

$$
\begin{aligned}
\Delta\tilde{\mathcal{H}}_{\mathrm{VN}}(\alpha_1,\alpha_2) &= \frac{1}{2n^2}\left\{\sum_{(u,v)\in\mathcal{E}}\frac{1}{d_u^{\mathrm{out}^2}}\left(\frac{(1-\alpha_2)cd_u^{\mathrm{in}}+\frac{1}{n}\frac{\alpha_2}{1+\alpha_2}}{(1-\alpha_2)cd_v^{\mathrm{in}}+\frac{1}{n}\frac{\alpha_2}{1+\alpha_2}}-\frac{(1-\alpha_1)cd_u^{\mathrm{in}}+\frac{1}{n}\frac{\alpha_1}{1+\alpha_1}}{(1-\alpha_1)cd_v^{\mathrm{in}}+\frac{1}{n}\frac{\alpha_1}{1+\alpha_1}}\right)\right\} \\
&= \frac{1}{2n^2}\left\{\sum_{(u,v)\in\mathcal{E}}\frac{1}{d_u^{\mathrm{out}^2}}\left(\frac{n(1-\alpha_2{}^2)cd_u^{\mathrm{in}}+\alpha_2}{n(1-\alpha_2{}^2)cd_v^{\mathrm{in}}+\alpha_2}-\frac{n(1-\alpha_1{}^2)cd_u^{\mathrm{in}}+\alpha_1}{n(1-\alpha_1{}^2)cd_v^{\mathrm{in}}+\alpha_1}\right)\right\} \\
&= \frac{1}{2n^2}\left\{\sum_{(u,v)\in E}\frac{1}{d_u^{\mathrm{out}^2}}\left(\frac{(n(1-\alpha_2{}^2)\alpha_1c(d_u^{\mathrm{in}}-d_v^{\mathrm{in}})-n(1-\alpha_1{}^2)\alpha_2c(d_u^{\mathrm{in}}-d_v^{\mathrm{in}})}{(n(1-\alpha_2{}^2)cd_v^{\mathrm{in}}+\alpha_2)(n(1-\alpha_1{}^2)cd_v^{\mathrm{in}}+\alpha_1)}\right)\right\} \\
&= \frac{1}{2n^2}\left\{\sum_{(u,v)\in\mathcal{E}}\frac{d_u^{\mathrm{in}}-d_v^{\mathrm{in}}}{d_u^{\mathrm{out}^2}}\left(\frac{nc(1-\alpha_2{}^2)\alpha_1-nc(1-\alpha_1{}^2)\alpha_2}{(n(1-\alpha_2{}^2)cd_v^{\mathrm{in}}+\alpha_2)(n(1-\alpha_1{}^2)cd_v^{\mathrm{in}}+\alpha_1)}\right)\right\} \\
&= \frac{1}{2n^2}\left\{\sum_{(u,v)\in\mathcal{E}}\frac{d_u^{\mathrm{in}}-d_v^{\mathrm{in}}}{d_u^{\mathrm{out}^2}}\left(\frac{nc(1/\alpha_2-\alpha_2)-nc(1/\alpha_1-\alpha_1)}{(n(1-\alpha_2{}^2)cd_v^{\mathrm{in}}+\alpha_2)(n(1-\alpha_1{}^2)cd_v^{\mathrm{in}}+\alpha_1)/(\alpha_1\alpha_2)}\right)\right\}.
\end{aligned}
\tag{6}
$$

Since $d_v^{\mathrm{in}} \leqslant n$ and $d_u^{\mathrm{out}} \leqslant n$,

$$
\begin{aligned}
\Delta\tilde{\mathcal{H}}_{\mathrm{VN}}(\alpha_1,\alpha_2) &\geqslant \frac{1}{2n^2}\sum_{(u,v)\in\mathcal{E}}(d_u^{\mathrm{in}}-d_v^{\mathrm{in}})\underbrace{\left(\frac{\frac{c}{n}(1/\alpha_2-\alpha_2-1/\alpha_1+\alpha_1)}{(n^2(1-\alpha_2{}^2)c+\alpha_2)(n^2(1-\alpha_1{}^2)c+\alpha_1)/(\alpha_1\alpha_2)}\right)}_{constant\ C} \\
&\geqslant \frac{C}{2n^2}\sum_{(u,v)\in\mathcal{E}}(d_u^{\mathrm{in}}-d_v^{\mathrm{in}}).
\end{aligned}
\tag{7}
$$

As $0 < \alpha_1 < \alpha_2 < 1$, the constant $C < 0$. And the edges point from node u to node v, thus the term $\sum_{(u,v)\in\mathcal{E}}(d_u^{\mathrm{in}} - d_v^{\mathrm{in}}) < 0$. Therefore,

$$\Delta\tilde{\mathcal{H}}_{\mathrm{VN}}(\alpha_1,\alpha_2) > 0. \tag{8}$$

Clearly, the perturbation error $\Delta\tilde{\mathcal{H}}_{\mathrm{VN}}$ increases monotonically with the Laplacian perturbation term $\Delta\alpha$. The proof is concluded. □

A.2 Proof of Theorems 2

THEOREM 2. *Bounds on the perturbation error*. *Given a directed graph $\mathcal{G} = (\mathcal{V},\mathcal{E})$ and the teleport probability α, the inequality*

$$0 < \Delta\tilde{\mathcal{H}}_{\mathrm{VN}}(\alpha,\alpha+\Delta\alpha) < \frac{1}{2n^2}\left\{\sum_{(u,v)\in\mathcal{E}}\left(\frac{1}{d_u^{out^2}}-\frac{\pi_{\mathrm{appr}}^{\alpha}(u)}{\pi_{\mathrm{appr}}^{\alpha}(v)d_u^{out^2}}\right)\right\} \tag{9}$$

holds. When the perturbation term $\Delta\alpha = 0$, $\Delta\tilde{\mathcal{H}}_{\mathrm{VN}} = 0$ and when $\Delta\alpha \to 1-\alpha$, the perturbation error $\Delta\tilde{\mathcal{H}}_{\mathrm{VN}}$ towards the upper bound.

Proof. From THEOREM 1, $\Delta\tilde{\mathcal{H}}_{\mathrm{VN}}$ increases monotonically with the Laplacian perturbation term $\Delta\alpha$. Thus, when $\Delta\alpha = 0$, $\Delta\tilde{\mathcal{H}}_{\mathrm{VN}} = 0$. For the upper bound of the perturbation error, we start with Eq. (2) that

$$(1-\alpha-\Delta\alpha)\pi_{\mathrm{appr}}^{\alpha+\Delta\alpha}\tilde{\mathbf{P}} + \frac{1}{n}\frac{\alpha+\Delta\alpha}{1+\alpha+\Delta\alpha}\mathbf{1}^{1\times n} = \pi_{\mathrm{appr}}^{\alpha+\Delta\alpha}. \tag{10}$$

Since π_{appr} is the stationary distribution and $\tilde{\mathbf{P}}$ is transition matrix, $\|\pi_{appr}\tilde{\mathbf{P}}\|_\infty \leqslant \|\pi_{appr}\|_\infty\|\tilde{\mathbf{P}}\|_\infty \leqslant 1$. It is easy to observe that when $\alpha+\Delta\alpha \to 1$, $\pi_{\mathrm{appr}}^{\alpha+\Delta\alpha} \to \frac{1}{2n}\mathbf{1}^{1\times n}$, which means $\pi_{\mathrm{appr}}^{\alpha+\Delta\alpha}(u), \pi_{\mathrm{appr}}^{\alpha+\Delta\alpha}(v)$ are equivalent as $\alpha + \Delta\alpha \to 1$. Thus,

$$\Delta\tilde{\mathcal{H}}_{\mathrm{VN}}(\alpha,\alpha+\Delta\alpha) \to \frac{1}{2n^2}\left\{\sum_{(u,v)\in\mathcal{E}}\left(\frac{1}{d_u^{\mathrm{out}^2}}-\frac{\pi_{\mathrm{appr}}^{\alpha}(u)}{\pi_{\mathrm{appr}}^{\alpha}(v)d_u^{\mathrm{out}^2}}\right)\right\}, \tag{11}$$

when $\alpha + \Delta\alpha \to 1$. The proof is concluded. □

B Supplementary Experiments

We will show here the supplementary experiments which are not described in the main text.

B.1 Experiments on the pacing function

Here, we provide more experiments on the pacing function. The pacing function determines in which order the contrastive views enter into the model. We want to know whether the information learned by the model in the easy contrastive view can help subsequent learning in the more difficult view.

Accuracy with epoch for different pacing functions. First, we give the results of the val accuracy changes with three different pacing functions in CORA-ML and AM-PHOTO in Figure 1(a) and 1(b) separately. We can find that different pacing functions perform differently at different training stages. Linear performs evenly throughout the training process; Exp improves faster at the beginning of training, but plateaus in the later stages; Log improves slowly at the beginning of training, but it continues to improve and achieves the best results at the end of training. The main reason is the log pacing function speeds up learning on easy tasks and stays on harder tasks for more epochs, helping the model to grasp the more subtle differences between contrastive views. This is the cause of its ability to consistently improve his performance in the later stages.

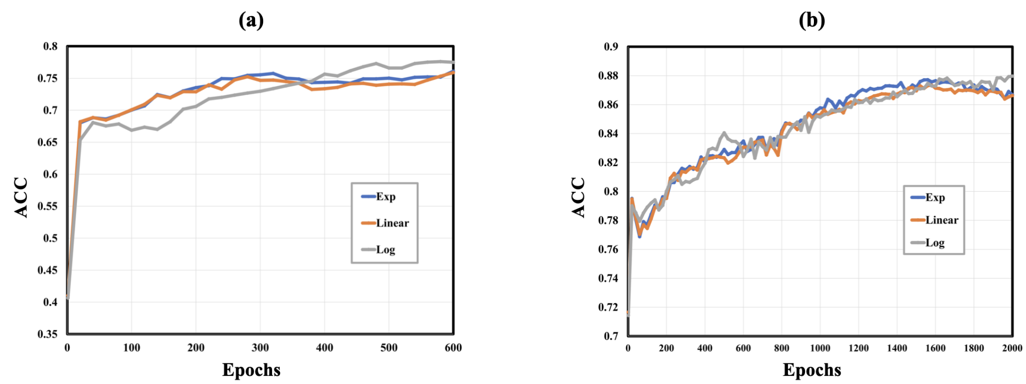

Figure 1: (a) performance of node classification task on CORA-ML with different pacing functions; (b) performance of node classification task on AM-PHOTO with different pacing functions.

Sensitivity analysis for initial and ending difficulty. Recalling the analysis in Section 3.2 of the main text, to obtain comprehensive contrastive information on the one hand, and to reduce the need for hyperparameters on the other hand, we set the initial perturbation term $\Delta\alpha_a$ to 0.8 and the ending perturbation term $\Delta\alpha_b$ to 0. In this experiment, we will explore the effect of different initial and ending difficulties on the accuracy of the model. We traverse the $\Delta\alpha_a, \Delta\alpha_b \in \{0, 0.1, 0.2, 0.3, 0.4, 0.5, 0.6, 0.7, 0.8\}$ and make sure $\Delta\alpha_a \geqslant \Delta\alpha_b$ ($\Delta\alpha_a = \Delta\alpha_b$ is equivalent to fixed view contrastive learning). We use two datasets and three pacing functions in the experiment. The results are shown in Figure 2. We can clearly find that setting the perturbation terms as the boundary values allows the model to learn all views as much as possible, thus improving the performance. Also, comparing the results of **Log**, **Liner**, and **Exp**, we can find that using log as the pacing function can get more stable and accurate results. This is consistent with the conclusion we obtain from the experiments in the main text.

From these experiments, we can draw a few empirical conclusions as follows.

- Log-based pacing function performs the best of the three pacing functions, but not too far from the other two pacing functions.
- The best results are obtained by setting the start and end points to be the boundary points of the Laplacian perturbation parameter space.
- The order in which the views are learned is crucial, with contrastive views working best from easy to difficult (Concluded from Table 1 in the main text).

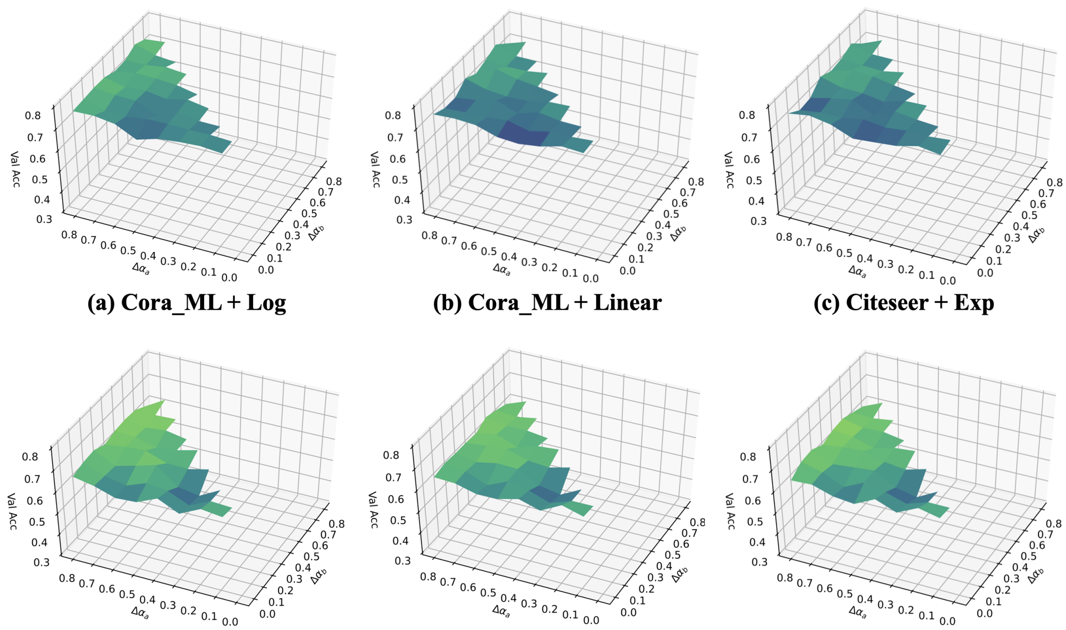

(a) Cora_ML + Log **(b) Cora_ML + Linear** **(c) Citeseer + Exp**

(d) Citeseer + Log **(e) Citeseer + Linear** **(f) Citeseer + Exp**

Figure 2: Validation accuracy of node classification task with different perturbation terms. The shade of the color represents the accuracy, with lighter shades indicating higher accuracy.

For the starting and ending difficulty scores, in accordance with the second conclusion, we consider that it is better to take the boundary values, which are effective and do not require parameter selection. For the type of pacing functions, according to the first and third conclusions, the different pacing functions have an impact on the results of the model but are not as important as the learning order. We believe that any pacing functions that satisfy the order of easy to difficult can be chosen.

C Reproducibility Details

To support the reproducibility of the results, in this paper, we detail the task, datasets, the baseline setting, and pseudocodes. We implement the DiGCL and all baseline models using the python library of PyTorch [2], Pytorch-Geometric [2] and DGL [17]. All the experiments are conducted on a server with one 12GB GPU (NVIDIA TITAN V), two CPUs (Intel Xeon E5 × 2) and Ubuntu 18.04 System.

C.1 Node Classification Task in Directed graphs

First, we define our task used in the main task as follow.

DEFINITION 1. ***Directed Graph Node Classification***. *Given a directed graph $\mathcal{G} = (\mathcal{V}, \mathcal{E})$ with adjacency matrix $\mathbf{A}$, and node feature matrix $\mathbf{X} \in \mathbb{R}^{n \times c}$, where $n = |\mathcal{V}|$ is the number of nodes and c is the feature dimension. Given a subset of nodes $\mathcal{V}_l \subset \mathcal{V}$, where nodes in $\mathcal{V}_l$ have observed labels and generally $|\mathcal{V}_l| << |\mathcal{V}|$. For semi-supervised (or supervised) methods, the task is using the labeled subset $\mathcal{V}_l$, node feature matrix $\mathbf{X}$ and adjacency matrix $\mathbf{A}$ predict the unknown label in $\mathcal{V}_{ul} = \mathcal{V} \setminus \mathcal{V}_l$. For self-supervised methods, the task requires to use the adjacency matrix $\mathbf{A}$ and the node feature matrix $\mathbf{X}$ to learn node representation without labels.*

Specifically, after the model has unsupervisedly learned the node feature representation, simple classical classification algorithms, such as logistic regression, SVM, and etc., can be used to categorize the nodes from the node representation, which is a semi-supervised step. In this paper, all experiments in semi-supervised learning are set up the same, including the division of the datasets and the number of trial repetitions.

[2] https://pytorch.org

C.2 Datasets Details

We use five open access datasets in the task of node classification. Label rate is the fraction of nodes in the training set per class. We use 20 labeled nodes per class to calculate the label rate.

Table 1: Datasets Details for Node Classification

Datasets	Graph type	Nodes	Edges	Classes	Features	Label rate
CORA-ML [1]	Directed Graphs	2995	8416	7	2879	4.67%
CITESEER [12]	Directed Graphs	3312	4715	6	3703	3.62%
AM-PHOTO [13]	Directed Graphs	7650	143663	8	745	2.10%
PUBMED [9]	Undirected Graphs	18230	79612	3	500	0.33%
DBLP [10]	Undirected Graphs	17716	105734	4	1639	0.45%

Besides, to verify the generalizability of our approach, we also perform the graph classification task on three undirected graph datasets in the experiments. We use the following: MUTAG [8] containing mutagenic compounds, PTC [8] containing compounds tested for carcinogenicity, and IMDB-BIN [18] connecting actors/actresses (nodes) based on movie appearances (edges).

Table 2: Datasets Details for Graph Classification

Datasets	Graphs	Average nodes per graph	Average edges per graph	Classes
MUTAG	188	17.93	19.79	2
PTC	344	14.29	14.69	2
IMDB-BIN	1000	19.77	193.06	2

C.3 Baselines Details and Settings

The baseline methods are given below:

Table 3: The hyperparameters of the baselines on node classification task.

Model	Training Type	Implementation
GCN [6]	Supervised	https://github.com/rusty1s/pytorch_geometric
GAT [15]	Supervised	
APPNP [7]	Supervised	
MagNet [21]	Supervised	https://github.com/matthew-hirn/magnet
DiGCN [14]	Supervised	https://github.com/flyingtango/DiGCN
DGI [16]	Self-supervised	https://github.com/PetarV-/DGI
GMI [11]	Self-supervised	https://github.com/zpeng27/GMI
MVGRL [4]	Self-supervised	https://github.com/kavehhassani/mvgrl
GraphCL [20]	Self-supervised	https://github.com/Shen-Lab/GraphCL
GRACE [22]	Self-supervised	https://github.com/CRIPAC-DIG/GRACE
GCA [23]	Self-supervised	https://github.com/CRIPAC-DIG/GCA

For all baseline models, we use their model structure in the original papers, including layer number, activation function selection, normalization and regularization selection, etc. We implement GCN, GAT, and APPNP using PyG [2]. Note that for DiGCN, we do not use its inception module but only use the directed graph convolution. Detailed hyper-parameter settings are shown in Table 4.

To ensure the generality of the model, we have minimized the variation of hyperparameters. Our implementation is based on the GRACE code, with improvements to the topological data augmentation and the model training scheme. For the feature-level perturbation part, we also apply the dropping feature method used in GCA, GRACE and MVGRL, with the same parameters as in GRACE. We initialize our model with Glorot initialization [3] and use Adam optimizer [5] in all datasets. The

Table 4: The hyperparameters of baselines for node classification task.

Model	layer	lr	weight-decay	hidden dimension	Others
GCN	2	0.01	5e-4	64	-
GAT	2	0.005	5e-4	CORA-ML & CITESEER:8 others:32	heads=16
APPNP	2	0.01	5e-4	64	$\alpha = 0.1$
MagNet	2	5e-3	5e-4	64	$K = 1, q = 0.1$
DiGCN	2	0.01	5e-4	64	$\alpha = 0.1$
DGI	1	0.001	0	512	max-LR-iter=150
GMI	1	0.001	0	512	$\alpha = 0.8, \beta = 1, \gamma = 1$
MVGRL	1	0.001	0	512	$\alpha = 0.2, t = 5$
GraphCL	1	0.001	0	512	drop rate=0.2
GRACE	2	0.001	1e-5	CORA-ML & CITESEER:128 others:256	augmentation parameters are consistent with the paper
GCA	2	0.001	1e-5	CORA-ML & CITESEER:128 others:256	augmentation parameters are consistent with the paper

initial learning rate is set to 0.001 and the weight decay factor is set to 1e-5 on all datasets. We set the number of layers used in the GCN encoder as 2. As stated in Section 3.2 of the main text, we fixed the initial and ending difficulty as 0.8 and 0 to obtain the complete contrastive information. The detailed parameter settings are shown in Table 5.

Table 5: The hyperparameters of our models.

Our models	layers	lr	weight-decay	hidden dimension	init $\Delta\alpha$	end $\Delta\alpha$	epochs
CORA-ML	2	0.001	1e-5	128	0.8	0	600
CITESEER	2	0.001	1e-5	128	0.8	0	300
AM-PHOTO	2	0.001	1e-5	512	0.8	0	2000
PUBMED	2	0.001	1e-5	256	0.8	0	600
DBLP	2	0.001	1e-5	256	0.8	0	600

For the graph classification task in the main text, we follow the setting in the [4] and only change the data augmentation and the pacing function. The hyperparameters are as follow.

Table 6: The hyperparameters on graph classification task.

Method	Hyperparameters	MUTAG	PTC	IMDB-BIN
MVGRL	layer	4	4	2
	batches	256	128	256
	epochs	20	20	20
	$\alpha = 0.2$	0.1	0.1	0.1
MVGRL+DiGCN	layer	4	4	2
	batches	256	128	256
	epochs	20	20	20
	$\Delta\alpha$	$0.8 \to 0$	$0.8 \to 0$	$0.8 \to 0$

C.4 Pseudocode

Here, we provide the pseudocode for two key algorithms, one for Laplacian perturbation proposed in Section 2 of the main text and the second for directed graph contrastive learning (DiGCL) introduced in Section 3 of the main text.

Algorithm 1: Laplacian Perturbation $\Phi(\cdot)$ Procedure

Input: Directed graph adjacency matrix: $\mathbf{A}$, teleport probability α, perturbation term $\Delta\alpha$
Output: Perturbed Laplacian $\hat{\mathbf{L}}_{\text{appr}}$

$\tilde{\mathbf{A}} \leftarrow \mathbf{A} + \mathbf{I}^{n\times n}$;
$\tilde{\mathbf{P}} \leftarrow \tilde{\mathbf{D}}^{-1}\tilde{\mathbf{A}}$;
$\hat{\alpha} = \alpha + \Delta\alpha$;
$\hat{\pi}_{\text{appr}} \leftarrow (1-\hat{\alpha})\hat{\pi}_{\text{appr}}\tilde{\mathbf{P}} + \frac{1}{n}\frac{\hat{\alpha}}{1+\hat{\alpha}}\mathbf{1}^{1\times n}$;
$\hat{\mathbf{\Pi}}_{\text{appr}} \leftarrow \frac{1}{\|\hat{\pi}_{\text{appr}}\|_1}\,\text{Diag}(\hat{\pi}_{\text{appr}})$;
$\hat{\mathbf{L}}_{\text{appr}} \leftarrow \mathbf{I} - \frac{1}{2}\left(\hat{\mathbf{\Pi}}_{\text{appr}}^{\frac{1}{2}}\tilde{\mathbf{P}}\hat{\mathbf{\Pi}}_{\text{appr}}^{-\frac{1}{2}} + \hat{\mathbf{\Pi}}_{\text{appr}}^{-\frac{1}{2}}\tilde{\mathbf{P}}^{T}\hat{\mathbf{\Pi}}_{\text{appr}}^{\frac{1}{2}}\right)$;
return $\hat{\mathbf{L}}_{\text{appr}}$

Algorithm 2: DiGCL Training Procedure

Input: Directed graph: $\mathcal{G}$, teleport probability α, scoring function: $\mathcal{D}$, pacing function: $\mathcal{P}$, encoder: $f^*(\cdot)$, projection head: $g(\cdot)$, data augmentation function: $\Phi(\cdot)$, loss function: $\ell(\cdot)$, number of iterations: L, initial difficulty d_a, ending difficulty d_b
Output: Trained Encoder $f^*(\cdot)$

Initialize $f^*(\cdot),\ g(\cdot)$;
for $l \leftarrow 0$ to L **do**
    $d_m = \mathcal{P}_{(d_a,d_b)}(l)$;
    $\Delta\alpha \leftarrow \mathcal{D}^{-1}(d_m)$;
    $U \leftarrow \mathbf{L}_{\text{appr}}(\mathcal{G},\alpha)$;
    $V \leftarrow \Phi_{\Delta\alpha}(\mathcal{G},\alpha)$;
    $\mathbf{H}_U \leftarrow f(U)$;
    $\mathbf{H}_V \leftarrow f(V)$;
    $\mathbf{Z}_U \leftarrow g(\mathbf{H}_U)$;
    $\mathbf{Z}_V \leftarrow g(\mathbf{H}_V)$;
    loss $\leftarrow \ell(\mathbf{Z}_U, \mathbf{Z}_V)$;
    SGD(loss) ;
end
return $f^*(\cdot)$

References

[1] A. Bojchevski and S. Günnemann, "Deep gaussian embedding of attributed graphs: Unsupervised inductive learning via ranking," *arXiv preprint arXiv:1707.03815*, 2017.

[2] M. Fey and J. E. Lenssen, "Fast graph representation learning with PyTorch Geometric," in *ICLR Workshop on Representation Learning on Graphs and Manifolds*, 2019.

[3] X. Glorot and Y. Bengio, "Understanding the difficulty of training deep feedforward neural networks," in *Proceedings of the thirteenth international conference on artificial intelligence and statistics*, 2010, pp. 249–256.

[4] K. Hassani and A. H. Khasahmadi, "Contrastive multi-view representation learning on graphs," *arXiv preprint arXiv:2006.05582*, 2020.

[5] D. P. Kingma and J. Ba, "Adam: A method for stochastic optimization," *Third ICLR*, 2015.

[6] T. N. Kipf and M. Welling, "Semi-supervised classification with graph convolutional networks," *arXiv preprint arXiv:1609.02907*, 2016.

[7] J. Klicpera, A. Bojchevski, and S. Günnemann, "Predict then propagate: Graph neural networks meet personalized pagerank," *arXiv preprint arXiv:1810.05997*, 2018.

[8] N. Kriege and P. Mutzel, "Subgraph matching kernels for attributed graphs," *arXiv preprint arXiv:1206.6483*, 2012.

[9] G. Namata, B. London, L. Getoor, B. Huang, and U. EDU, "Query-driven active surveying for collective classification," in *10th International Workshop on Mining and Learning with Graphs*, vol. 8, 2012.

[10] S. Pan, J. Wu, X. Zhu, C. Zhang, and Y. Wang, "Tri-party deep network representation," *Network*, vol. 11, no. 9, p. 12, 2016.

[11] Z. Peng, W. Huang, M. Luo, Q. Zheng, Y. Rong, T. Xu, and J. Huang, "Graph representation learning via graphical mutual information maximization," in *Proceedings of The Web Conference 2020*, 2020, pp. 259–270.

[12] P. Sen, G. Namata, M. Bilgic, L. Getoor, B. Galligher, and T. Eliassi-Rad, "Collective classification in network data," *AI magazine*, vol. 29, no. 3, pp. 93–93, 2008.

[13] O. Shchur, M. Mumme, A. Bojchevski, and S. Günnemann, "Pitfalls of graph neural network evaluation," *arXiv preprint arXiv:1811.05868*, 2018.

[14] Z. Tong, Y. Liang, C. Sun, X. Li, D. Rosenblum, and A. Lim, "Digraph inception convolutional networks," *Advances in Neural Information Processing Systems*, vol. 33, 2020.

[15] P. Veličković, G. Cucurull, A. Casanova, A. Romero, P. Lio, and Y. Bengio, "Graph attention networks," *arXiv preprint arXiv:1710.10903*, 2017.

[16] P. Veličković, W. Fedus, W. L. Hamilton, P. Liò, Y. Bengio, and R. D. Hjelm, "Deep graph infomax," *arXiv preprint arXiv:1809.10341*, 2018.

[17] M. Wang, L. Yu, D. Zheng, Q. Gan, Y. Gai, Z. Ye, M. Li, J. Zhou, Q. Huang, C. Ma, Z. Huang, Q. Guo, H. Zhang, H. Lin, J. Zhao, J. Li, A. J. Smola, and Z. Zhang, "Deep graph library: Towards efficient and scalable deep learning on graphs," *ICLR Workshop on Representation Learning on Graphs and Manifolds*, 2019. [Online]. Available: https://arxiv.org/abs/1909.01315

[18] P. Yanardag and S. Vishwanathan, "Deep graph kernels," in *Proceedings of the 21th ACM SIGKDD international conference on knowledge discovery and data mining*, 2015, pp. 1365–1374.

[19] C. Ye, R. C. Wilson, C. H. Comin, L. d. F. Costa, and E. R. Hancock, "Approximate von neumann entropy for directed graphs," *Physical Review E*, vol. 89, no. 5, p. 052804, 2014.

[20] Y. You, T. Chen, Y. Sui, T. Chen, Z. Wang, and Y. Shen, "Graph contrastive learning with augmentations," *Advances in Neural Information Processing Systems*, vol. 33, 2020.

[21] X. Zhang, N. Brugnone, M. Perlmutter, and M. Hirn, "Magnet: A magnetic neural network for directed graphs," *arXiv preprint arXiv:2102.11391*, 2021.

[22] Y. Zhu, Y. Xu, F. Yu, Q. Liu, S. Wu, and L. Wang, "Deep graph contrastive representation learning," *arXiv preprint arXiv:2006.04131*, 2020.

[23] Y. Zhu, Y. Xu, F. Yu, Q. Liu, S. Wu, and L. Wang, "Graph contrastive learning with adaptive augmentation," *arXiv preprint arXiv:2010.14945*, 2020.